ANALYSING TRACER RETURNS FROM GEOTHERMAL RESERVOIRS

Graham Weir and John Burnell[1]

[1]GNS, 1 Fairway Drive, Avalon, Lower Hutt 5010, New Zealand

G.Weir@GNS.cri.nz

Keywords: *geothermal field, tracer profiles, first arrival time, peak arrival time, tail, percentage recovery.*

ABSTRACT

Tracer returns provide direct proof of fluid connections between different wells in a geothermal field. The tracer profile yields estimates for travel times and fluid recovery fractions between injection and production wells, and can provide strong constraints on assumed reservoir structure in numerical simulators. Analysis of tracer profiles is not always straightforward, due to uncertainties from secondary injection of tracer, and from assumptions about the "tracer tail". In addition, the mechanism of tracer transport involves many effects such as pressure gradients in the reservoir, tending to move tracer from injector to producer; negative buoyancy effects due to cold injection which tend to move tracer vertically downwards; and the structure of fracture and matrix system. The importance of each of these effects will vary in different geothermal fields.

We briefly discuss several standard methods of tracer analysis, and then focus on an alternative method of tracer analysis, which may be of value for tracer profiles characterised by long tails. We use a class of remarkable probability functions which have unbounded moments (mean, variance, etc). The method cannot be applied universally to all tracer profiles, but does provide an idealised framework for a general classification of tracer profiles, and in many cases, may yield improved estimates for the fraction of tracer recovered. We test this method with field data.

1. INTRODUCTION

Tracer measurements have been used in producing geothermal fields over the last 30 years [Stefansson, 1997] to identify flow connections and travel times of tracer between injection and producing wells. Types of tracer used include: fluorescent dyes (rodamine, sodium fluorescein, tinopal), inert gases (Xe, sodium hexafluoride), organic compounds (aromatic acids), radioactive isotopes (Xe133, I125, I131), naturally occurring chemicals (NaCl), and alcohol (methanol, ethanol) tracers [Bixley et al, 1995],[Rose et al, 2001],[Adams et al, 2000].

Tracer measurements are especially important in geothermal fields where injection is occurring. If rapid and significant tracer returns are observed between injection and production wells, then injection from these wells may need to be stopped or moved to elsewhere in the field because of the potential threat of cold returns to production wells.

Transport of tracer results primarily from flow dispersion (spatial variation in velocity), and diffusion, through an immense number of flow paths, the nature of which are unknown. If density effects due to temperature differences are important, as is likely about injection wells, relative depths of feed points in injection and producer wells will also be important. Additionally, nearby producers may capture tracer, hiding connections between wells. These and other complexities show that the interpretation of tracer profiles should proceed cautiously, given the difficult and unknown aspects of much of the flow geometry relevant to tracer returns.

Tracer measurements record the rate of recovered tracer versus time. Typical inferences from such tracer datasets include first arrival time, peak arrival time, and percentage recovery of total injected tracer.

Several methods are used to analyse tracer returns, including: the mean residence time method; the fractional derivative method; the travel-time method; the fracture block method; the convolution method; the non-parametric method, and numerical simulation.

The mean residence time method [Shook, 2005] uses the first moment of the tracer data, to provide a characteristic time for the tracer record. This method works in principle, provided the first moment is bounded. The fractional derivative method [Suzuki et al., 2010] assumes non-Fickian mass transport. The travel-time method [Bullivant and OSullivan, 1991] aims to locate geological structures such as faults. The fracture block method [Jensen and Horne, 1983] assumes two permeability structures to explain aspects of fast and slow transport in geothermal fields. The convolution method [Yanigasawa et al, 2009] calculates secondary and higher tracer returns, adding these to the primary tracer returns, to improve estimates of tracer recovery. The non-parametric method [Villacorte et al., 2010] aims to obtain unbiased estimates of well to well connectivity. Numerical simulation [Nakao et al., 2007] is perhaps the most robust of methods, because it aims to describe in detail the porous medium connecting injection and production wells. Below we discuss a new parametric method, which attempts to capture the scale dependence seen in many porous flow measurements.

2. THE METHOD

This section considers an idealized tracer concentration, C, imagined to result from the instantaneous injection of a given mass of tracer at the injector, measured at the producer, with all mass flow rates held constant.

$$C = \frac{\rho f x}{q\sqrt{2\pi\sigma t^2}} \exp[-(\frac{x-ut}{\sqrt{2\sigma t}})^2] \qquad (1)$$

Here C is wellhead tracer concentration (kg/m^3), ρ is producer water density (kg/m^3), f mass variable (kg), x nominal distance between injector and producer (m), q producer flow rate (kg/s), σ diffusion parameter (m^2/s^2), t time (s), and u is nominal fluid speed (m/s) between wells.

This expression attempts to describe tracer transport with a speed u, and a diffusion coefficient that increases linearly time (D=σt). Using diffusivities which increase with system size, has been suggested previously [Neuman, 1990].

The peak concentration in (1) occurs when

$$\frac{x}{u} = \left(\frac{1+\sqrt{1+4\alpha}}{2}\right) t_m \; ; \; \alpha = \frac{2\sigma}{u^2} \qquad (2)$$

which allows x to be replaced by the peak time, t_m. If (2) is substituted into (1), and C is scaled by the peak concentration C_m, then the tracer profile is a function of t/t_m and α, where α is non-dimensional (= 2/Peclet number).

$$\frac{C}{C_m} = \frac{t_m^2}{t^2} \exp\left[\frac{(\sqrt{1+4\alpha}-1)^2}{4\alpha}\right] \exp\text{-}\left[\frac{[(\sqrt{1+4\alpha}+1)\frac{t_m}{2t}-1]^2}{\alpha}\right] \quad (3)$$

Equation (3) may be useful, since both C_m and t_m can be read off the tracer plot, and then α is determined from (3).

The total mass M of tracer recovered (kg) is

$$M = \int_0^\infty \frac{qC}{\rho}\, dt = \frac{f}{2}\left[1 + erf\left(\frac{1}{\sqrt{\alpha}}\right)\right] \qquad (4)$$

where erf is the error function, and (4) is independent of x. Then (4) can be rewritten, using the non-dimensional R, as

$$M = \frac{\mathrm{R}\, \mathrm{q}\, C_m\, t_m}{\rho} \qquad (5)$$

where R is given in Table 1. Note that M = f when α=0, but then $C_m = \infty$, explaining why R is zero then.

Table 1.Variation of R in (5) with α.

α	R	α	R	α	R
0.0	0.0	0.8	1.383	7.0	2.054
0.01	0.177	0.9	1.434	8.0	2.077
0.1	0.558	1.0	1.479	9.0	2.097
0.2	0.783	2.0	1.739	10.0	2.113
0.4	1.071	3.0	1.861	50.0	2.279
0.5	1.172	4.0	1.936	100	2.318
0.6	1.255	5.0	1.987	1000	2.381
0.7	1.324	6.0	2.024	∞	$\frac{\sqrt{\pi}e}{2} = 2.409$

Table 2. First inflection point times, as a function of α. The ratio t_1/t_m equals $1/\sqrt{3}$ when α = ∞, and 0 for α = 0.

α	t_1/t_m	α	t_1/t_m	α	t_1/t_m
0.1	0.2353	0.8	0.3994	7.0	0.5073
0.2	0.2920	0.9	0.4073	10.0	0.5179
0.3	0.3252	1.0	0.4142	50.0	0.5498
0.4	0.3482	2.0	0.4548	100.0	0.5578
0.5	0.3653	3.0	0.4745	1000.0	0.5711
0.6	0.3789	4.0	0.4869	10,000	0.5754
0.7	0.3900	5.0	0.4956	∞	0.5774

Table 2 tabulates t_1, the time of the first inflection point for Equation (3). The first arrival time t_0 , given in Table 3, is

$$t_0 = t_1 - \frac{C(t_1)}{\dot{c}(t_1)} \qquad (6)$$

where $\dot{c}(t_1)$ is the time derivative of C at $t = t_1$.

Table 3. First arrival times, as a function of α.

α	t_m/t_0	α	t_m/t_0	α	t_m/t_0
0.0	1.0	0.7	1.817	7.0	2.131
0.01	1.144	0.8	1.842	10.0	2.159
0.1	1.428	0.9	1.863	50.0	2.241
0.2	1.563	1.0	1.882	100.0	2.261
0.3	1.646	2.0	1.992	1000.0	2.294
0.4	1.706	3.0	2.045	10,000.0	2.305
0.5	1.751	4.0	2.078	∞	2.309
0.6	1.787	5.0	2.100	∞	$4/\sqrt{3}$

Table 3 shows that (3) requires the peak arrival times to vary between 1 and 2.3 times the first arrival time. Numerous tracer plots have been published over the years, and are referenced in the IGA Website Database, under tracer conference papers. There are examples in this database which support Table 3, but not every example follows Table 3. In some cases, there is not a clear first arrival time, and instead a gradual increase in tracer concentration is recorded.

The special case of (3) for very large α is

$$\frac{C}{C_m} = \frac{et_m^2}{t^2} \exp\left(-\frac{t_m^2}{t^2}\right) \; ; \; \alpha = \infty \qquad (7)$$

3. APPLICATIONS OF THE METHOD

Figure 1 plots the concentration calculated from (7), and an approximation to a published tracer plot from the Raft River geothermal field in 2010 [Mattson et al., 2011]. The model does not match the peak tracer concentration, but after this, (7) closely follows the data.

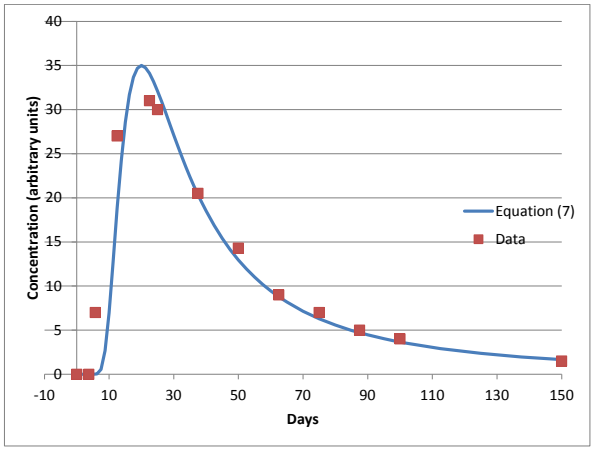

Figure 1: RRG-1, Raft river, Cassia County, Idaho, 2010 [Mattson et al., 2011].

While a relatively small, but significant number of published tracer plots can be approximated by (7), a greater proportion

of tracer plots can be approximated by (3). The tracer plot from WK121 [McCabe, et al., 1983] in July 1979, from the Wairakei geothermal field in New Zealand, is given in Figure 2 for α equal to 0.85.

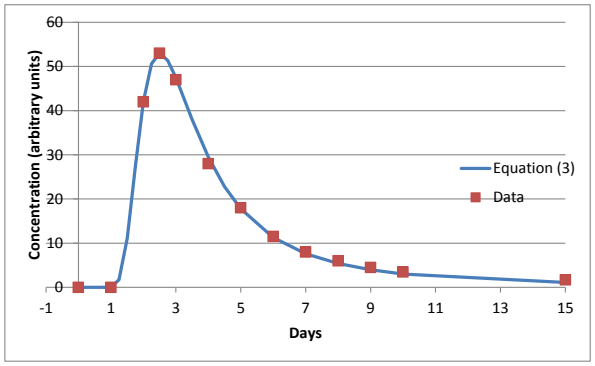

Figure 2: WK121 response to WK101, July 1979, Wairakei. Fitted Equation (3) has α = 0.85.

It is surprising that (3) can approximate, crudely at least, a large number of tracer profiles. Specifically, once (3) has been adjusted to pass through the peak in the tracer plot, then there is only one parameter (α) left in the fitting. There is a maximum "width" that can be tolerated, corresponding to an infinite value of α.

Figure 2 is unusual for tracer profiles, since the "first returns" are apparent for many multiples of t_m. More usually, tracer returns from secondary reinjection will reach the producer well, and may provide a confusing background flow. A possible example of this is shown in Figure 3, from well SG-6 in the Svartsengi field in Iceland [Gudmundsson and Hauksson, 1985].

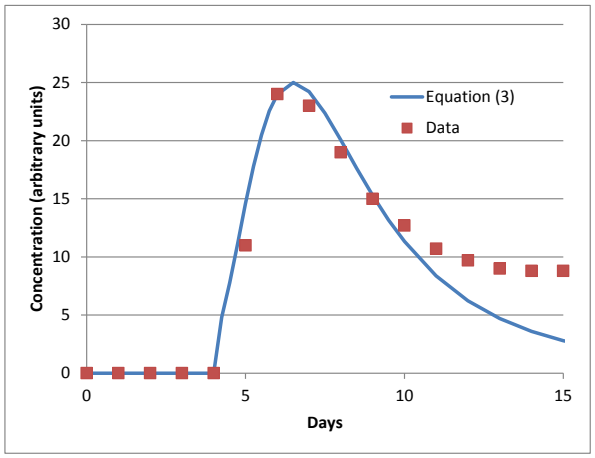

Figure 3: Tracer curve from SG-6, Svartsengi field, Iceland, 1985. Fitted Equation (3) has α = 0.3.

4. TOTAL TRACER RETURNS

An immediate challenge is to determine the tail of the tracer return plot, from amongst what are likely to be a background of tracer readings. Here we will not do this for actual field data, because we do not know the total mass flowing to the producer from the initial injection of tracer.

Rather, we will consider the case when the actual tracer profile from the producer is assumed to be that from (7), and that the background flows become apparent at $2t_m$. In a field in which reinjection is occurring, it is reasonable to expect a significant mass of secondary tracer to have arrived by $2t_m$, since t_m is a crude estimate to the time for tracer to move from injector to producer, provided the time to return fluid from the producer to the power plant and back to the injector, is small relative to t_m. Figure 3 shows a departure between fitted and measured values at about $2t_m$.

For simplicity, we take $q/\rho = 1 = t_m$, C_m=1, and consider the infinite α case in (7). Then all methods should yield the total mass of tracer recovered up to time $2t_m$ as $(e\sqrt{\pi}\ \mathrm{erfc}(0.5))/2$, or 1.155, where erfc is the complementary error function. The total mass of tracer recovered equals $(e\sqrt{\pi})/2 = 2.409$, and so the total mass in the tail beyond $2t_m$ equals 1.254.

But if a decreasing exponential function is matched to (7) at time $2t_m$, it will be C = 0.25 exp(2.25-0.75t), and the mass in the tail will equal 0.706. Consequently, this apparently quite reasonable analysis approach will estimate the total mass recovered as 1.861= 1.155+0.706, which is only 77% of the mass recovered of 2.409.

Alternatively, from (4) and (7), for infinite α, the mass of tracer in the tail after time t, MT(t), is

$$MT(t) = \frac{e\sqrt{\pi}}{2}\frac{qC_m t_m}{\rho}\,\mathrm{erf}\left(\frac{t_m}{t}\right) \qquad (8)$$

where erf is the error function. Consequently, the fraction of the mass of tracer remaining in the tail at time t is

$$\frac{MT(t)}{MT(0)} = \mathrm{erf}\left(\frac{t_m}{t}\right) \approx \frac{2t_m}{t\sqrt{\pi}} \qquad (9)$$

for small t_m/t. From (9), 10% of the total mass of tracer to be recovered, remains in the tail at $t = 11t_m$, for α=∞.

The equations above assume implicitly that the measured tracer profiles can be adequately approximated by (3). While this appears to be true for a significant number of tracer plots, it is also untrue for a significant number of tracer plots. Of course, in these cases, the selection into true/untrue is subjective.

The equation for C in (3) has the property that for small α, C is essentially a delta function, but as α increases towards infinity, the width of C increases, but only to the extent of being described by (7). Many tracer plots are clearly much wider than constrained by (7), and so cannot be fitted by (3). For example, corresponding to Figure 2, the tracer responses in July 1979 from injection at WK101, at producers WK103, WK116 and WK76 are too wide to be fitted by (3). There are many other examples of tracer returns whose broad peaks are too wide to be fitted by (3).

Additionally, there are also examples where different assumptions above do not hold in actual tracer tests. For example, tracer tests have occurred during times of significant changes to flow rate, due to field management, contradicting the assumption that q is constant. In other cases, variable flow rates occur naturally from cycling in multi-feed wells.

Another example where (3) is not applicable is for injection-backflow tracer tests, where tracer is first injected, and then produced from the same well [Kocabas and Horne, 1987].

5. CONCLUSIONS

This paper has introduced a theoretical tracer profile, with a very long tail. Instead of the usual eventual exponential decay with time, as characterized by finite variance distributions, (3) eventually decays as t^{-2}. Consequently,

(3) will typically predict higher rates of tracer recovery, than for methods based on profiles with a finite variance.

An "obvious" estimate for the mass of tracer in the tail, was shown in a plausible example above, to be an underestimate of the mass of tracer recovered by 23%.

This significant difference in the two estimates for tracer recovery is closely related to the very long tail for (3) and (7), since (9) showed that 10% of the total tracer recovered still resides in the tail at $t = 11t_m$. In many cases, tracer records will not extend out to such long times.

These two issues of possible significant underestimation of tracer recovery, and of the very long possible tracer tails, can perhaps be dismissed by arguing that (3) cannot apply to tracer profiles, since there are many examples where (3) does not apply. Countering this viewpoint are examples where (3) does appear to hold, as in Figures 1 and 2.

In those cases where secondary tracer returns from injection are confusing the tracer profile, it seems to be an open question whether the tracer tail decays exponentially or algebraically with time. While exponential decay is widely assumed, we have highlighted some of the consequences if the tracer tail decays algebraically, instead.

Finally, tracer returns can be classified as obeying (3), or not. If (3), then:

1. Tracer returns are classified by percentage recovery, peak time, peak value, and α;
2. The mean residence time method is inapplicable, and will be characterized by extremely sensitive results when considering the tracer tail [Grant and Bixley, 2011];
3. Traditional methods can underestimate percentage recovery, perhaps by around 20%, when secondary returns are important;
4. The tracer tail will decay as the inverse square of time;
5. All moments (apart from the zero moment) of the tracer profile are unbounded;
6. The ratio of peak to first arrival times varies between 1 and 2.3;
7. Up to 10% of the total tracer recovered may remain in the tail, after 11 times the peak time;
8. The limiting case of infinite α provides strong constraints on the applicability of (3).

REFERENCES

Adams, M.C., Yamada, Y, Yagi, M. Kondo, T. and Wada, T. Stability of Methanol, Propanol and SF6 as High temperature Tracers, Proc. World Geothermal Congress, 3015 – 3019, 2000.

Bixley, P.F., Glover, R.B., McCabe, W.J., Barry, B.J. and Jordan, J.T., Tracer Calibration tests at Wairakei geothermal field, Proc. World Geothermal Congress, 1887 – 1891, 1995.

Bullivant, D.P. and OSullivan, M.J., Travel time analysis of Tracer tests in two geothermal fields, Transport in Porous Media, 6, 241 – 259, 1991.

Grant, M.A. and Bixley, P.F., Geothermal Reservoir Engineering, 2nd Edition, Academic Press, 2011.

Gudmusson, J.S. and Hauksson, T., Tracer survey in Svartsengi field 1984, Transactions Geothermal Resources Council, 9(2), 307-315, 1985.

Jensen, C.L. and Horne, R.N., Matrix diffusion and its effect on the modelling of tracer returns from the fractured geothermal reservoir at Wairakei, New Zealand, Proc. Ninth Workshop Geothermal Reservoir Engineering, Stanford University, Stanford, California, Dec 1983, 323 – 329.

Kocabas, I. and Horne, R.N., Analysis of Injection-Backflow Tracer Tests in Fractured Geothermal Reservoirs, Proc. 12th Workshop on Geothermal Reservoir Engineering, Stanford University, Stanford, California, SGP-Tr-109, Jan 20-22, 1987.

Mattson, E., Plummer, M., Palmer, C., Hull, L., Miller, S., and Nye, R., Comparison of three tracer tests at the Raft River Geothermal Site, Proc. 36th Workshop on Geothermal Reservoir Engineering, Stanford University, Stanford, California, SGP-Tr-191, Jan 31- Feb 2, 2011.

McCabe, W.J., Barry, B.J. and Manning, M.R., Radioactive tracers in geothermal underground water flow studies, Geothermics, Vol. 12, No. 2/3, pp 83 – 110, 1983.

Nakao, S., Ishido, T. and Takahashi, Y. Numerical simulation of tracer testing data at the Uenotai geothermal field, Japan. Proc. 32nd Workshop on Geothermal Reservoir Engineering, Stanford University, Stanford, 207 – 212, 2007.

Neuman, S.P., Universal scaling of hydraulic conductivities and dispersivities in geologic media, Water Resources Research, 26, 1949-1758, 1990.

Rose, P.E., Benoit, W.R. and Kilbourn, P.M., The application of the polyaromatic sulfonates as tracers in geothermal reservoirs, Geothermics, 30, 617 – 640, 2001.

Shook, G.M., A systematic method for tracer test analysis: an example using Beowawe tracer data. Proc. 30th Workshop on Geothermal Reservoir Engineering, Stanford University, Stanford, California, 166-171, 2005.

Stefansson, V., Geothermal Reinjection Experience, Geothermics Vol 26 No. 1, pp 99 – 139, 1997.

Suzuki, A., Chiba, R., Okaze, T., Nibori, Y., Fomin, S., Chugnov, V. and Hashida, T., Characterising non-Fickian transport in fractured rock masses using fractional derivative-based mathematical model, GRC Transactions, 34, 1179 – 1184, 2010.

Villacorte, J.D., Malate, R.C.M. and Horne, R.N., Application of Nonparametric Regression on Well Histories of Geothermal Production Fields in the Philippines, Proc. World Geothermal Congress, Bali, Indonesia, 1 – 5, 25 – 29 April, 2010.

Yanagisawa, N., Rose, P. and Wyborn, D., First tracer test at CooperBasin, Australia HDR Reservoir, GRC Transactions, 33, 281 – 284, 2009.